UNIVERSITY *of* York

This is a repository copy of *Climatic controls of decomposition drive the global biogeography of forest-tree symbioses*.

White Rose Research Online URL for this paper:
https://eprints.whiterose.ac.uk/148523/

Version: Accepted Version

Article:

(2019) Climatic controls of decomposition drive the global biogeography of forest-tree symbioses. Nature. pp. 404-408. ISSN 0028-0836

https://doi.org/10.1038/s41586-019-1128-0

White Rose
university consortium
Universities of Leeds, Sheffield & York

eprints@whiterose.ac.uk
https://eprints.whiterose.ac.uk/

Title: Climatic controls of decomposition drive the global biogeography of forest tree symbioses

Authors: *Steidinger BS[1]*, Crowther TW[2]†*, Liang J†[3,4]*, Van Nuland ME[1], Werner GDA[5], Reich PB[6,7], Nabuurs G[8], de-Miguel S[9,10], Zhou M[3], Picard N[11], Herault B[12], Zhao X[4], Zhang C[4], Routh D[2], [GFBi Author List], and Peay KG[1]†*

Affiliations:
[1] Department of Biology, Stanford University, Stanford CA USA
[2] Department of Environmental Systems Science, ETH Zürich, Zürich, Switzerland
[3] Department of Forestry and Natural Resources, Purdue University, West Lafayette, IN, USA
[4] Research Center of Forest Management Engineering of State Forestry Administration, Beijing Forestry University, Beijing, China
[5] Department of Zoology, University of Oxford, Oxford UK
[6] Department of Forest Resources, University of Minnesota
[7] Hawkesbury Institute for the Environment, Western Sydney University
[8] Wageningen University and Research
[9] Departament de Producció Vegetal i Ciència Forestal, Universitat de Lleida-Agrotecnio Center
[10] Forest Science and Technology Centre of Catalonia (CTFC)
[11] Food and Agriculture Organization of the United Nations
[12] Cirad, INP-HB, Univ Montpellier, UPR Forêts et Sociétés

*These authors contributed equally to this work and share the first-author
†Corresponding authors: Email kpeay@stanford.edu; albeca.liang@gmail.com; tom.crowther@usys.ethz.ch

GFBi Author List

Meinrad Abegg [1], Yves Adou Yao [2], Giorgio Alberti [3], Angelica Almeyda Zambrano [4], Esteban Alvarez-Davila [5], Patricia Alvarez-Loayza [6], Luciana F. Alves [7], Christian Ammer [8], Clara Antón-Fernández [9], Alejandro Araujo-Murakami [10], Luzmila Arroyo [11], Valerio Avitabile [12], Gerardo Aymard [13], Timothy Baker [14], Radomir Bałazy[15], Olaf Banki [16], Jorcely Barroso [17], Meredith Bastian [18], Jean-Francois Bastin [19], Luca Birigazzi [20], Philippe Birnbaum [21], Robert Bitariho [22], Pascal Boeckx [23], Frans Bongers [24], Olivier Bouriaud [25], Pedro Brancalion [26], Susanne Brandl [27], Francis Q. Brearley [28], Roel Brienen [29], Eben Broadbent [30], Helge Bruelheide [31], Filippo Bussotti [32], Roberto Cazzolla Gatti [33], Ricardo Cesar [34], Goran Cesljar [35], Robin Chazdon [36], Han Y. H. Chen [37], Chelsea Chisholm [38], Emil Cienciala [39], Connie J. Clark [40], David Clark [41], Gabriel Colletta [42], Richard Condit [43], David Coomes [44], Fernando Cornejo Valverde [45], Jose J. Corral-Rivas [46], Philip Crim [47], Jonathan Cumming [48], Selvadurai Dayanandan [49], André L. de Gasper [50], Mathieu Decuyper [51], Géraldine Derroire [52], Ben DeVries [53], Ilija Djordjevic [54], Amaral Iêda [55], Aurélie Dourdain [56], Nestor Laurier Engone Obiang [57], Brian Enquist [58], Teresa Eyre [59], Adandé Belarmain Fandohan [60], Tom M. Fayle [61], Ted R. Feldpausch [62], Leena Finér [63], Markus Fischer [64], Christine

Fletcher [65], Jonas Fridman [66], Lorenzo Frizzera [67], Javier G. P. Gamarra [68], Damiano Gianelle [69], Henry B. Glick [70], David Harris [71], Andrew Hector [72], Andreas Hemp [73], Geerten Hengeveld [74], John Herbohn [75], Martin Herold [76], Annika Hillers [77], Eurídice N. Honorio Coronado [78], Markus Huber [79], Cang Hui [80], Kook Jo Hyun [81], Thomas Ibanez [82], Bin Jung Il [83], Nobuo Imai [84], Andrzej M. Jagodzinski [85], Bogdan Jaroszewicz [86], Vivian Johannsen [87], Carlos A. Joly [88], Tommaso Jucker [89], Viktor Karminov [90], Kuswata Kartawinata [91], Elizabeth Kearsley [92], David Kenfack [93], Deborah Kennard [94], Sebastian Kepfer-Rojas [95], Gunnar Keppel [96], Mohammed Latif Khan [97], Timothy Killeen [98], Hyun Seok Kim [99], Kanehiro Kitayama [100], Michael Köhl [101], Henn Korjus [102], Florian Kraxner [103], Diana Laarmann [104], Mait Lang [105], Simon Lewis [106], Huicui Lu [107], Natalia Lukina [108], Brian Maitner [109], Yadvinder Malhi [110], Eric Marcon [111], Beatriz Marimon [112], Ben Hur Marimon-Junior [113], Andrew Robert Marshall [114], Emanuel Martin [115], Olga Martynenko [116], Jorge A. Meave [117], Omar Melo-Cruz [118], Casimiro Mendoza [119], Cory Merow [120], Abel Monteagudo Mendoza [121], Vanessa Moreno [122], Sharif A. Mukul [123], Philip Mundhenk [124], Maria G. Nava-Miranda [125], David Neill [126], Victor Neldner [127], Radovan Nevenic [128], Michael Ngugi [129], Pascal Niklaus [130], Jacek Oleksyn [131], Petr Ontikov [132], Edgar Ortiz-Malavasi [133], Yude Pan [134], Alain Paquette [135], Alexander Parada Gutierrez [136], Elena Parfenova [137], Minjee Park [138], Marc Parren [139], Narayanaswamy Parthasarathy [140], Pablo L. Peri [141], Sebastian Pfautsch [142], Oliver Phillips [143], Maria Teresa Piedade [144], Daniel Piotto [145], Nigel C. A. Pitman [146], Irina Polo [147], Lourens Poorter [148], Axel Dalberg Poulsen [149], John R. Poulsen [150], Hans Pretzsch [151], Freddy Ramirez Arevalo [152], Zorayda Restrepo-Correa [153], Mirco Rodeghiero [154], Samir Rolim [155], Anand Roopsind [156], Francesco Rovero [157], Ervan Rutishauser [158], Purabi Saikia [159], Philippe Saner [160], Peter Schall [161], Mart-Jan Schelhaas [162], Dmitry Schepaschenko [163], Michael Scherer-Lorenzen [164], Bernhard Schmid [165], Jochen Schöngart [166], Eric Searle [167], Vladimír Seben [168], Josep M. Serra-Diaz [169], Anatoly Shvidenko [170], Javier Silva-Espejo [171], Marcos Silveira [172], James Singh [173], Plinio Sist [174], Ferry Slik [175], Bonaventure Sonké [176], Alexandre F. Souza [177], Krzysztof Stereńczak [178], Jens-Christian Svenning [179], Miroslav Svoboda [180], Natalia Targhetta [181], Nadja Tchebakova [182], Hans ter Steege [183], Raquel Thomas [184], Elena Tikhonova [185], Peter Umunay [186], Vladimir Usoltsev [187], Fernando Valladares [188], Fons van der Plas [189], Tran Van Do [190], Rodolfo Vasquez Martinez [191], Hans Verbeeck [192], Helder Viana [193], Simone Vieira [194], Klaus von Gadow [195], Hua-Feng Wang [196], James Watson [197], Bertil Westerlund [198], Susan Wiser [199], Florian Wittmann [200], Verginia Wortel [201], Roderick Zagt [202], Tomasz Zawila-Niedzwiecki [203], Zhi-Xin Zhu [204], Irie Casimir Zo-Bi [205]

GFBi Author Affiliations

[1] WSL Swiss Federal Institute for Forest, Snow and Landscape Research, Birmensdorf, Switzerland
[2] UFR Biosciences, University Félix Houphouët-Boigny, Côte d'Ivoire
[3] Department of Agricultural, Food, Environmental and Animal Sciences, University of Udine, 33100 Udine, Italy; Istitute of Biometeorology, National Research Council (CNR-IBIMET), 50145 Firenze, Italy

88 [4] Spatial Ecology and Conservation Lab, Department of Tourism, Recreation and Sport
89 Management, University of Florida, Gainesville, Florida, 32611 USA
90 [5] Universidad Nacional Abierta y a Distancia, UNAD; Fundacion ConVida, Medellin,
91 Colombia
92 [6] Field Museum of Natural History, 1400 Lake Shore Drive, Chicago, IL 60605, USA,
93 [7] Center for Tropical Research, Institute of the Environment and Sustainability, UCLA, USA
94 [8] Silviculture and Forest Ecology of the Temperate Zones, University of Göttingen, Germany
95 [9] Division of Forest and Forest Resources. Norwegian Institute of Bioeconomy Research
96 (NIBIO), Norway
97 [10] Museo de Historia Natural Noel Kempff Mercado, Universidad Autonoma Gabriel Rene
98 Moreno, Santa Cruz de la Sierra, Bolivia
99 [11] Museo de Historia Natural Noel Kempff Mercado, Universidad Autonoma Gabriel Rene
100 Moreno, Santa Cruz de la Sierra, Bolivia
101 [12] European Commission, Joint Research Centre, Ispra, Italy; Wageningen University &
102 Research, Netherlands
103 [13] UNELLEZ-Guanare, Programa de Ciencias del Agro y el Mar, Herbario Universitario
104 (PORT), Portuguesa 3323, Venezuela
105 [14] School of Geography, University of Leeds, UK
106 [15] Department of Geomatics, Forest Research Institute, Braci Leśnej 3 Street, Sękocin Stary,
107 05-090 Raszyn, Poland
108 [16] Naturalis Biodiversity Centre, Darwinweg 2, 2333 CR Leiden, Netherlands
109 [17] Universidade Federal do Acre, Campus Floresta, Cruzeiro do Sul, Acre, Brazil
110 [18] Smithsonian's National Zoo, 3001 Connecticut Ave NW, Washington, DC 20008, USA
111 [19] Institute of Integrative Biology, ETH Zurich, Univeritätstrasse 16, 8092, Switzerland
112 [20] Food and Agriculture Organization of the United Nations, Rome, Italy
113 [21] Centre de coopération internationale en recherche agronomique pour le développement,
114 France
115 [22] Institute of Tropical Forest Conservation, Mbarara University of Sciences and Technology,
116 Mbarara, Uganda
117 [23] Ghent University, Isotope Bioscience Laboratory - ISOFYS, Coupure Links 653, 9000
118 Gent, Belgium
119 [24] Wageningen University & Research, PO Box 47, 6700AA Wageningen, Netherlands
120 [25] Stefan cel Mare University of Suceava, Strada Universității 13, Suceava 720229, Romania
121 [26] Department of Forest Sciences, Luiz de Queiroz College of Agriculture, University of São
122 Paulo, Piracicaba, SP 13418-900, Brazil
123 [27] Bavarian State Institute of Forestry, Hans-Carl-von-Carlowitz-Platz 1, Freising 85354,
124 Germany
125 [28] Manchester Metropolitan University, UK
126 [29] School of Geography, University of Leeds, UK
127 [30] Spatial Ecology and Conservation Lab, School of Forest Resources and Conservation,
128 University of Florida, Gainesville, Florida, 32611 USA
129 [31] Institute of Biology Geobotany and Botanical Garden, Martin Luther University Halle-
130 Wittenberg & German Centre for Integrative Biodiversity Research (iDiv) Halle-Jena-Leipzig,
131 Germany
132 [32] University of Firenze. Department of Agriculture, Food, Environment and Forest (DAGRI).
133 Piazzale delle Cascine 28, 50144 Firenze. Italy

134 [33] Biological Institute, Tomsk State University, Tomsk, 634050 Russia; Department of
135 Forestry and Natural Resources, Purdue University, West Lafayette, Indiana, 47907 USA
136 [34] Department of Forest Sciences, Luiz de Queiroz College of Agriculture, University of São
137 Paulo, Piracicaba, SP 13418-900. Brazil
138 [35] Department of Spatial regulation, GIS and Forest Policy, Institute of Forestry, Kneza
139 Višeslava 3, 11030 Beograd, Srbija
140 [36] University of Connecticut, Department of Ecology and Evolutionary Biology, Storrs, CT
141 06268-3043 USA; University of the Sunshine Coast, Tropical Forests and People Research
142 Centre, Maroochydore, Queensland, Australia
143 [37] Faculty of Natural Resources Management, Lakehead University, Thunder Bay, Ontario,
144 Canada, P7B 5E1; Key Laboratory for Humid Subtropical Eco-Geographical Processes of the
145 Ministry of Education, Fujian Normal University, Fuzhou, China, 350007
146 [38] Center for Macroecology, Evolution and Climate, Natural History Museum of Denmark,
147 University of Copenhagen, Universitetsparken 15, 2100 Copenhagen, Denmark
148 [39] IFER - Institute of Forest Ecosystem Research, Jilove u Prahy; Global Change Research
149 Institute CAS, Brno, Czech Republic
150 [40] Nicholas School of the Environment, Duke University, NC USA
151 [41] Department of Biology, University of Missouri-St. Louis, St. Louis, MO USA
152 [42] Department of Plant BIology, Institute of Biology, University of Campinas, UNICAMP,
153 Brazil
154 [43] Smithsonian Tropical Research Institute, Apartado 0843-03092, Balboa, Ancon, Panama
155 [44] Department of Plant Sciences, University of Cambridge, Downing Street, Cambridge, CB2
156 3EA, UK
157 [45] Andes to Amazon Biodiversity Program, Madre de Dios, Madre de Dios, Peru
158 [46] Facultad de Ciencias Forestales, Universidad Juárez del Estado de Durango, Mexico
159 [47] School of Mathematics and Sciences, The College of Saint Rose, Albany, NY, 12205, USA;
160 Department of Biology, West Virginia University, Morgantown, WV, 26506, USA
161 [48] Department of Biology, West Virginia University, Morgantown, WV, 26501, USA
162 [49] Biology Department, Concordia University, L-SP 445-01, Loyola Campus7141, Sherbrooke
163 Street W. Montreal, Quebec, Canada
164 [50] Natural Science Department, Universidade Regional de Blumenau, Brazil
165 [51] Laboratory of Geo-Information Science and Remote Sensing, Wageningen University &
166 Research; Forest Ecology and Forest Management Group, Wageningen University & Research,
167 Netherlands
168 [52] Cirad, UMR EcoFoG (AgroParistech, CNRS, Inra, Université des Antilles, Université de la
169 Guyane), Campus Agronomique, Kourou, French Guiana
170 [53] Department of Geographical Sciences, University of Maryland, USA
171 [54] Institute of Forestry, Serbia
172 [55] National Institut Research Amazon, Brazil
173 [56] Cirad, UMR EcoFoG (AgroParistech, CNRS, Inra, Université des Antilles, Université de la
174 Guyane), Campus Agronomique, Kourou, French Guiana
175 [57] IRET, Herbier National du Gabon (CENAREST), Libreville, Gabon
176 [58] Department of Ecology and Evolutionary Biology, University of Arizona, Tucson, AZ,
177 85719, USA; The Santa Fe Institute, Santa Fe, New Mexico, 87501, USA
178 [59] Queensland Herbarium, Department of Environment and Science, Australia
179 [60] Ecole de Foresterie et Ingénierie du Bois, Université Nationale d'Agriculture, Bénin

4

[61] Biology Centre of the Czech Academy of Sciences, Institute of Entomology, Branisovska 31, 370 05 Ceske Budejovice, Czech Republic

[62] Geography, College of Life and Environmental Sciences, University of Exeter, Exeter, UK

[63] Natural Resources Institute, Latokartanonkaari 9 FI-00790, Helsinki, Finland

[64] Institute of Plant Sciences, University of Bern, Hochschulstrasse 6, 3012 Bern, Switzerland

[65] Forest Research Institute Malaysia, Jalan Frim, Kepong, 52109 Kuala Lumpur, Selangor, Malaysia

[66] Department of Forest Resource Management, Swedish University of Agricultural Sciences SLU, Sweden

[67] Department of Sustainable Agro-Ecosystems and Bioresources, Research and Innovation Center, Fondazione Edmund Mach di San Michele all'Adige, Via E. Mach, 1 38010 S. Michele all'Adige (TN), Italy

[68] Food and Agriculture Organization of the United Nations, Viale delle Terme di Caracalla, 00153 Rome, Italy

[69] Department of Sustainable Agro-Ecosystems and Bioresources, Research and Innovation Center, Fondazione Edmund Mach di San Michele all'Adige, Via E. Mach, 1 38010 S. Michele all'Adige (TN), Italy

[70] Yale University, School of Forestry and Environmental Studies, CT, USA

[71] Royal Botanic Garden Edinburgh, 20A Inverleith Row, Edinburgh EH3 5LR, Scotland, UK

[72] University of Oxford, Department of Plant Sciences, OX1 3RB, Oxford, UK

[73] University of Bayreuth, Department of Plant Systematics, Universitätsstrasse 30, 95447 Bayreuth, Germany

[74] Wageningen Univeristy and Research, 6708 PB Wageningen, Netherlands

[75] Tropical Forests and Peopel Research Centre, University of the Sunshine Coast, Maroochydore DC, Queensland 4558, Australia

[76] Laboratory for Geoinformation Science and Remote Sensing, Wageningen University, 6708 PB Wageningen, Netherlands

[77] The Royal Society for the Protection of Birds, Sandy, UK

[78] Instituto de Investigaciones de la Amazonía Peruana, Av. José Abelardo Quiñones km 2.5, Iquitos, Peru

[79] WSL Swiss Federal Institute for Forest, Snow and Landscape Research, Switzerland

[80] Centre for Invasion Biology, Department of Mathematical Sciences, Stellenbosch University, Matieland 7602, South Africa;Theoretical Ecology Unit, African Institute for Mathematical Sciences, Cape Town 7945, South Africa

[81] Forest Resources Information Division, Korea Forest Promotion Institute, South Korea

[82] Institut Agronomique néo-Calédonien (IAC), Equipe Sol & Végétation (SolVeg), BPA5, 98800 Nouméa, New Caledonia

[83] Forest Resources Information Division, Korea Forest Promotion Institute, South Korea

[84] Department of Forest Science, Tokyo University of Agriculture, Japan

[85] Institute of Dendrology, Polish Academy of Sciences, Parkowa 5, 62-035 Kórnik, Poland; Poznań University of Life Sciences, Department of Game Management and Forest Protection, Wojska Polskiego 71c, 60-625 Poznań, Poland

[86 Bialowieza Geobotanical Station, Faculty of Biology, University of Warsaw, Sportowa 19, 17-230 Białowieża, Poland

[87] Department of Geosciences and Natural Resource Management, University of Copenhagen, Nørregade 10, 1165 København, Denmark

226 [88] Plant Biology Department, Biology Institute, State University of Campinas, UNICAMP,
227 Campinas, SP, 13083-862, Brazil [ORCID # 0000-0002-7945-2805]
228 [89] CSIRO Land and Water, Centre for Environment and Life Sciences, Floreat, WA, 6014
229 Australia
230 [90] Bauman Moscow State Technical University, Russia
231 [91] Integrative Research Center, the Field Museum of Natural History, 1400 Lake Shore Drive,
232 Chicago, IL 60605, USA
233 [92] Centre for the Research and Technology of Agro-Environmental and Biological Sciences,
234 CITAB; University of Trás-os-Montes and Alto Douro, UTAD; Escola Superior Agrária de
235 Viseu, Portugal
236 [93] CTFS-ForestGEO, Smithsonian Tropical Research Institute, Apartado 0843-03092, Balboa,
237 Ancon, Panama
238 [94] Department of Physical and Environmental Sciences, Colorado Mesa University, 1100
239 North Ave, Grand Junction, CO 81501, USA
240 [95] Department of Geosciences and Natural Resource Management, University of Copenhagen,
241 Nørregade 10, 1165 København, Denmark
242 [96] School of Natural and Built Environments and Future Industries Institute, University of
243 South Australia, GPO Box 2471, Adelaide, SA 5001
244 [97] Department of Botany, Dr. Harisingh Gour Central University, Sagar - 470003, MP, India
245 [98] Museo de Historia Natural Noel Kempff Mercado, Universidad Autonoma Gabriel Rene
246 Moreno, Santa Cruz de la Sierra, Bolivia
247 [99] Department of Forest Sciences, Seoul National University, Seoul 08826, Republic of Korea;
248 Interdisciplinary Program in Agricultural and Forest Meteorology, Seoul National University,
249 Seoul 08826, Republic of Korea; National Center for Agro Meteorology, Seoul 08826, Republic
250 of Korea; Research Institute for Agriculture and Life Sciences, Seoul National University, Seoul
251 08826, Republic of Korea
252 [100] Graduate School of Agriculture, Kyoto University, Yoshidahonmachi, Sakyo Ward,
253 Kyoto, Kyoto Prefecture 606-8501, Japan
254 [101] Institute for World Forestry, University of Hamburg, Mittelweg 177 20148 Hamburg
255 Germany
256 [102] Institute of Forestry and Rural Engineering, Estonian University of Life Sciences,
257 Friedrich Reinhold Kreutzwaldi 1, 51014 Tartu, Estonia
258 [103] International Institute for Applied Systems Analysis, Laxenburg, Austria
259 [104] Institute of Forestry and Rural Engineering, Estonian University of Life Sciences,
260 Friedrich Reinhold Kreutzwaldi 1, 51014 Tartu, Estonia
261 [105] Institute of Forestry and Rural Engineering, Estonian University of Life Sciences,
262 Friedrich Reinhold Kreutzwaldi 1, 51014 Tartu, Estonia
263 [106] School of Geography University of Leeds, UK; Department of Geography, University
264 College London, UK
265 [107] Faculty of Forestry, Qingdao Agricultural University, 700 Changcheng Rd, Chengyang
266 Qu, Qingdao Shi, Shandong Sheng, China
267 [108] Center for Forest Ecology and Productivity RAS, ul. Profsoyuznaya 84, 32, Russia
268 [109] Department of Ecology and Evolutionary Biology, University of Arizona, Tucson, AZ,
269 85719, USA
270 [110] School of Geography, University of Oxford, UK

271 [111] UMR EcoFoG, AgroParisTech, CNRS, Cirad, INRA, Université des Antilles, Université
272 de Guyane, French Guiana
273 [112] Departamento de Ciências Biológicas, Universidade do Estado de Mato Grosso, Nova
274 Xavantina, Brazil
275 [113] Departamento de Ciências Biológicas, Universidade do Estado de Mato Grosso, Nova
276 Xavantina, Brazil
277 [114] Tropical Forests and People Research Centre, University of the Sunshine Coast,
278 Queensland, Australia; Department of Environment & Geography, University of York, UK;
279 Flamingo Land Ltd., North Yorkshire, UK
280 [115] Department of Wildlife Management, College of African Wildlife Management, Mweka,
281 Tanzania
282 [116] Forestry Faculty, Bauman Moscow State Technical University, 2-Ya Baumanskaya Ulitsa,
283 д.5, стр.1, Moskva 105005, Russia
284 [117] Departamento de Ecología y Recursos Naturales, Facultad de Ciencias, Universidad
285 Nacional Autónoma de México, Mexico
286 [118] Universidad del Tolima, Ibagué, Colombia
287 [119] Colegio de Profesionales Forestales de Cochabamba, Cochabamba, Bolivia
288 [120] Ecology and Evolutionary Biology, University of Connecticut, Storrs 06269, CT, USA
289 [121] Jardín Botánico de Missouri, Oxapampa, Peru, Universidad Nacional de San Antonio
290 Abad del Cusco, Peru
291 [122] Department of Forest Sciences, Luiz de Queiroz College of Agriculture, University of São
292 Paulo, Piracicaba, SP 13418-900. Brazil
293 [123] Department of Enviornmental Management, School of Environmental Science and
294 Management, Independent University Bangladesh, Dhaka 1229, Bangladesh; Tropical Forests
295 and People Research Centre, University of the Sunshine Coast, Maroochydore DC, Queensland
296 4558, Australia
297 [124] Institute for World Forestry, University of Hamburg, Germany
298 [125] Instituto de Silvicultura e Industria de la Madera, Universidad Juárez del Estado de
299 Durango, Mexico
300 [126] Universidad Estatal Amazónica, Puyo, Pastaza, Ecuador
301 [127] Department of Environment and Science, Queensland Herbarium, Mount Coot Tha Rd,
302 Toowong QLD 4066, Australia
303 [128] Institute of Forestry Belgrade, Serbia
304 [129] Department of Environment and Science, Queensland Herbarium, Mount Coot Tha Rd,
305 Toowong QLD 4066, Australia
306 [130] Department of Evolutionary Biology and Environmental Studies, University of Zurich,
307 Winterthurerstrasse 190, CH-8057 Zurich, Switzerland
308 [131] Polish Academy of Sciences, Institute of Dendrology, Parkowa 5, PL-62-035 Kórnik,
309 Poland; Department of Forest Resources, University of Minnesota, St. Paul, MN, USA
310 [132] Bauman Moscow State Technical University, 2-Ya Baumanskaya Ulitsa, д.5, стр.1,
311 Moskva 105005, Russia
312 [133] Forestry School. Instituto Tecnologico de Costa Rica. Cartago P.O. 159-7050, Costa Rica
313 [134] USDA Forest Service, USA
314 [135] Université du Québec à Montréal, Département des sciences biologiques and Centre for
315 Forest Research, PO Box 8888, Centre-ville Station, Montréal, Qc, Canada H3C 3P8

[136] Museo de Historia Natural Noel Kempff Mercado, Universidad Autonoma Gabriel Rene Moreno, Santa Cruz de la Sierra, Bolivia

[137] V.N.Sukachev Institute of Forest of FRC KSC SB RAS, Russia

[138] Department of Forest Sciences, Seoul National University, Seoul 08826, Republic of Korea; Urban Forests Research Center, National Institute of Forest Science, Seoul 02455, Republic of Korea

[139] Wageningen University and Research, 6708 PB Wageningen, Netherlands

[140] Department of Ecology and Environmental Sciences, Pondicherry University, India

[141] Instituto Nacional de Tecnología Agropecuaria (INTA), Universidad Nacional de la Patagonia Austral (UNPA), Consejo Nacional de Investigaciones Científicas y Tecnicas (CONICET), Argentina

[142] School of Social Sciences and Psychology (Urban Studies), Western Sydney University, Locked Bag 1797, Penrith, NSW 2751, Australia

[143] University of Leeds, School of Geography, U.K.

[144] Instituto Nacional de Pesquisas da Amazônia, Brazil

[145] Laboratório de Dendrologia e Silvicultura Tropical, Centro de Formação em Ciências Agroflorestais, Universidade Federal do Sul da Bahia

[146] Field Museum of Natural History, 1400 Lake Shore Drive, Chicago, IL 60605, USA

[147] Jardín Botánico de Medellín, Cl. 73 #51d14, Medellín, Antioquia, Colombia

[148] Wageningen University and Research, 6708 PB Wageningen, Netherlands

[149] Royal Botanic Garden Edinburgh, Arboretum Pl, Edinburgh EH3 5NZ, UK

[150] Nicholas School of the Environment, Duke University, 9 Circuit Dr, Durham, NC 27710, USA

[151] Chair for Forest Growth and Yield Science, TUM School for Life Sciences, Technical University of Munich, Germany

[152] Universidad Nacional de la Amazonía Peruana, Sargento Lores 385 Iquitos, Loreto, Peru

[153] Corporacion COL-TREE; Facultad de Ingeniera Ambinetal, Universidad de Antioquia, Colombia

[154] Department of Sustainable Agro-Ecosystems and Bioresources, Research and Innovation Center, Fondazione Edmund Mach; Agriculture, Food and Environment Centre (C3A), University of Trento, San Michele all`Adige, Italy.

[155] Colaborador do Laboratório de Dendrologia e Silvicultura Tropical, Centro de Formação em Ciências Agroflorestais, Universidade Federal do Sul da Bahia

[156] Department of Biological Sciences, Boise State University, ID, USA

[157] Tropical Biodiversity Section, MUSE - Museo delle Scienze, Trento, Italy; Department of Biology, University of Florence, Florence, Italy

[158] Smithsonian Tropical Research Institute, Apartado 0843-03092, Balboa, Ancon, Panama

[159] Department of Environmental Sciences, Central University of Jharkhand, Brambe-835205, Ranchi, Jharkhand, India

[160] University of Zurich, Rämistrasse 71, 8006 Zurich, Switzerland

[161] Silviculture and Forest Ecology of the Temperate Zones, University of Göttingen, Germany

[162] Wageningen University and Research, 6708 PB Wageningen, Netherlands

[163] International Institute for Applied Systems Analysis, Laxenburg, Austria

[164] Faculty of Biology, Geobotany, University of Freiburg, Fahnenbergplatz, 79085 Freiburg im Breisgau, Germany

362   [165] University of Zurich, Rämistrasse 71, 8006 Zurich, Switzerland
363   [166] Instituto Nacional de Pesquisas da Amazônia, Av. André Araújo 2936, 69067-375 Manaus,
364   Brazil
365   [167] Faculty of Natural Resources Management, Lakehead University, Thunder Bay, Ontario,
366   P7B 5E1, Canada
367   [168] National Forest Centre, Forest Research Institute Zvolen, T. G. Masaryka 2175, 22, SK -
368   960 92, Zvolen
369   [169] Université de Lorraine, AgroParisTech, Inra, Silva, 54000, Nancy, France; Center for
370   Biodiversity Dynamics in a Changing World (BIOCHANGE), Department of Bioscience,
371   Aarhus University
372   [170] International Institute for Applied Systems Analysis, Laxenburg, Austria
373   [171] Departamento de Biología, Universidad de la Serena, Casilla 554, La Serena, Chile
374   [172] Universidade Federal do Acre, Rio Branco, Brazil
375   [173] Guyana Forestry Commission, Georgetown, Guiana
376   [174] CIRAD, UPR Forests&Societies, Univ. Montpellier
377   [175] Environmental and Live Sciences, Faculty of Science, Universiti Brunei Darussalam, Jalan
378   Tungku Link, Gadong, BE1410, Brunei Darussalam
379   [176] Plant Systematic and Ecology Laboratory, Department of Biology, University of Yaounde
380   [177] Departamento de Ecologia, Universidade Federal do Rio Grande do Norte, Natal, Brazil
381   [178] Department of Geomatics, Forest Research Institute, Braci Leśnej 3 Street, Sękocin Stary,
382   05-090 Raszyn, Poland
383   [179] Center for Biodiversity Dynamics in a Changing World (BIOCHANGE), Department of
384   Bioscience, Aarhus University; Section for Ecoinformatics & Biodiversity, Department of
385   Bioscience, Aarhus University
386   [180] Faculty of Forestry and Wood Sciences, Czech University of Life Sciences Prague,
387   Kamýcká 129, Praha 6 Suchdol 16521, Czech Republic
388   [181] Instituto Nacional de Pesquisas da Amazônia, Av. André Araújo, 2936 - Petrópolis,
389   Manaus - AM, 69067-375, Brazil
390   [182] V.N.Sukachev Institute of Forest of FRC KSC SB RAS, 50, Akademgorodok,
391   Krasnoyarsk, 660036, Siberia
392   [183] Naturalis Biodiversity Center, Leiden, The Netherlands & Systems Ecology, Free
393   University Amsterdam, Netherlands
394   [184] Iwokrama International Centre for Rainforest Conservation and Development (IIC),
395   Georgetown, Guiana
396   [185] Center for Forest Ecology and Productivity, Russian Academy of Sciences
397   [186] School of Forestry and Environmental Studies, Yale University, 195 Prospect St, New
398   Haven, CT 06511, USA
399   [187] Botanical Garden of Ural Branch of Russian Academy of Sciences, Ural State Forest
400   Engineering University, Ekaterinburg, Russia
401   [188] Museo Nacional de Ciencias Naturales, Calle de José Gutiérrez Abascal, 2, 28006 Madrid,
402   Spain
403   [189] Systematic Botany and Functional Biodiversity, Institute of Biology, Leipzig University,
404   Germany
405   [190] Silviculture Research Institute, Vietnamese Academy of Forest Sciences, Duc Thang, Bac
406   Tu Liem, Hanoi, Vietnam
407   [191] Jardín Botánico de Missouri, Peru

408 [192] Ghent University, St. Pietersnieuwstraat 33, 9000 Gent, Belgium
409 [193] Centre for the Research and Technology of Agro-Environmental and Biological Sciences,
410 CITAB, University of Trás-os-Montes and Alto Douro, UTAD, Portugal. Escola Superior
411 Agrária de Viseu.
412 [194] Environmental Studies and Research Center, University of Campinas, Rua dos
413 Flamboyants, 155, Campinas, SP 13083-867, Brazil.
414 [195] Extraordinary Professor Department of Forest and Wood Science, University of
415 Stellenbosch, South Africa
416 [196] Key Laboratory of Tropical Biological Resources, Ministry of Education, Hainan
417 University, Haikou, Hainan 570228, China
418 [197] Division of Forestry and Natural Resources, West Virginia University, USA
419 [198] Department of Forest Resource Management, Swedish University of Agricultural Sciences
420 SLU, Sweden
421 [199] Manaaki Whenua -- Landcare Research, Lincoln 7640, New Zealand
422 [200] Department of Wetland Ecology, Institute for Geography and Geoecology, Karlsruhe
423 Institute for Technology, Germany
424 [201] Centre for Agricultural Research in Suriname (CELOS), Suriname
425 [202] Tropenbios International, P.O.Box 232, 6700 AE Wageningen, Netherlands
426 [203] Polish State Forests, Coordination Center for Environmental Projects, Poland
427 [204] Institute of Tropical Agriculture and Forestry, Hainan University, Haikou, Hainan, China
428 [205] Department of Forestry and Environment, National Polytechnic Institute (INP-HB),
429 Yamoussoukro, Côte d'Ivoire
430

431 **Manuscript**

432   **The identity of the dominant microbial symbionts in a forest determines the ability**

433 **of trees to access limiting nutrients from atmospheric or soil pools[1,2], sequester**

434 **carbon[3,4] and withstand the impacts of climate change[1-6]. Characterizing the global**

435 **distribution of symbioses, and identifying the factors that control it, are thus integral to**

436 **understanding present and future forest ecosystem functioning. Here we generate the first**

437 **spatially explicit global map of forest symbiotic status using a database of over 1.1 million**

438 **forest inventory plots with over 28,000 tree species. Our analyses indicate that climatic**

439 **variables, and in particular climatically-controlled variation in decomposition rate, are the**

440 **primary drivers of the global distribution of major symbioses. We estimate that**

441 **ectomycorrhizal (EM) trees, which represent only 2% of all plant species[7], constitute**

approximately 60% of tree stems on Earth. EM symbiosis dominates forests where seasonally cold and dry climates inhibit decomposition, and are the predominant symbiosis at high latitudes and elevation. In contrast, arbuscular mycorrhizal (AM) trees dominate aseasonally warm tropical forests and occur with EM trees in temperate biomes where seasonally warm-and-wet climates enhance decomposition. Continental transitions between AM and EM dominated forests occur relatively abruptly along climate driven decomposition gradients, which is likely caused by positive plant-microbe feedbacks. Symbiotic N-fixers, which are insensitive to climatic controls on decomposition compared with mycorrhizal fungi, are most abundant in arid biomes with alkaline soils and high maximum temperatures. The climatically driven global symbiosis gradient we document represents the first spatially-explicit, quantitative understanding of microbial symbioses at the global scale and demonstrates the critical role of microbial mutualisms in shaping the distribution of plant species.

Microbial symbionts strongly influence the functioning of forest ecosystems. They exploit inorganic, organic[2] and/or atmospheric forms of nutrients that enable plant growth[1], determine how trees respond to elevated CO_2[6], regulate the respiratory activity of soil microbes[3,8], and affect plant species diversity by altering the strength of conspecific negative density dependence[9]. Despite growing recognition of the importance of root symbioses for forest functioning[1,6,10] and the potential to integrate symbiotic status into Earth system models that predict functional changes to the terrestrial biosphere[10], we lack spatially-explicit, quantitative maps of the different root symbioses at the global scale. Generating these quantitative maps of tree symbiotic states would link the biogeography of functional traits of belowground microbial

464 symbionts with their 3.1 trillion host trees[11], spread across Earth's forests, woodlands, and

465 savannas.

466   The dominant guilds of tree root symbionts, arbuscular mycorrhizal (AM) fungi,

467 ectomycorrhizal (EM) fungi, ericoid mycorrhizal (ErM) fungi, and nitrogen (N)-fixing bacteria

468 (N-fixer) are all based on the exchange of plant photosynthate for limiting macronutrients. The

469 AM symbiosis evolved nearly 500 million years ago, with EM, ErM and N-fixer plant taxa

470 evolving multiple times from an AM basal state. Plants that form the AM symbiosis comprise

471 nearly 80% of all terrestrial plant species, and principally rely on AM fungi for enhancing

472 mineral phosphorus (P) uptake[12]. In contrast to AM fungi, EM fungi evolved from multiple

473 lineages of saprotrophic ancestors, and as a result some EM fungi are more capable of mobilizing

474 organic sources of soil nutrients (particularly nitrogen)[2]. Association with EM fungi, but not AM

475 fungi, has been shown to allow trees to accelerate photosynthesis in response to increased

476 atmospheric CO_2 when soil nitrogen (N) is limiting[6] and to inhibit soil respiration by decomposer

477 microbes[3,8]. Because increased plant photosynthesis and decreased soil respiration both reduce

478 atmospheric CO_2 concentrations, the EM symbiosis is associated with buffering the Earth's

479 climate against anthropogenic changes.

480   In contrast to mycorrhizal fungi, which extract nutrients from the soil, symbiotic N-fixers

481 (Rhizobia and Actinobacteria) convert atmospheric N_2 to plant-usable forms. Symbiotic N-fixers

482 are responsible for a large fraction of biological soil-N inputs, which can increase N-availability

483 in forests where they are locally abundant[13]. Both N-fixing bacteria and EM fungi often demand

484 more plant photosynthate than does the AM symbiosis[12,14,15]. Because tree growth and

485 reproduction are limited by access to inorganic, organic and atmospheric sources of N, the

486 distribution of root symbioses is likely to reflect both environmental conditions that maximize

487   the cost-benefit ratio of symbiotic exchange as well as physiological constraints on different

488   symbionts.

489   In one of the earliest efforts to understand the functional biogeography of plant root

490   symbioses, Sir David Read[16] categorically classified biomes by their perceived dominant

491   mycorrhizal type and hypothesized that seasonal climates favor hosts associating with EM fungi

492   due to their ability to compete directly for organic N. In contrast, it has been proposed that

493   sensitivity to low temperatures has prevented N-fixers from dominating outside the tropics,

494   despite the potential for N-fixation to alleviate N-limitation in boreal forests[15,17]. However,

495   global scale tests of these proposed biogeographic patterns and their climate drivers are lacking.

496   To address this research gap, we compiled the first global ground-sourced survey database to

497   reveal numerical abundances of each symbiosis across the globe, which is essential for

498   identifying the potential mechanisms underlying transitions in forest symbiotic state along

499   climatic gradients[18,19].

500   We determined the abundance of tree symbioses using GFBi, an extension from the plot-

501   based Global Forest Biodiversity (GFB) database, which contains over 1.1 million forest

502   inventory plots of individual-based measurement records from which we derive abundance

503   information for entire tree communities (Figure 1). Using published literature on the

504   evolutionary histories of mycorrhizal and N-fixer symbioses, we assigned plant species from the

505   GFBi to one of 5 symbiotic guilds: AM, EM, ErM, N-fixer, and non- or weakly-mycorrhizal

506   (NM). We then used the random forest algorithm with K-fold cross validation to determine the

507   importance and influence of variables related to climate, soil chemistry, vegetation, and

508   topography on the relative abundance of each tree-symbiotic guild (Figure 2). Because

509   decomposition is the dominant process by which soil nutrients become available to plants, we

510 calculated annual and quarterly decomposition coefficients according to the Yasso07 model[20],

511 which describes how temperature and precipitation gradients influence mass-loss rates of

512 different chemical pools of leaf litter (with parameters fit using a previous global study of leaf

513 decomposition, Figures 3, S5). Finally, we projected our predictive models across the globe over

514 the extent global biomes that fell within the multivariate distribution of our model training data

515 (Figures 4, S14-15, see Methods for full description).

516   Our analysis shows that the three most numerically abundant tree symbiotic guilds each

517 have reliable environmental signatures, with the four most important predictors accounting for

518 81, 79, and 52% of the total variability in EM, AM, and N-fixer relative basal area, respectively.

519 Models for ErM and NM lack strong predictive power given the relative rarity of these symbiotic

520 states amongst trees, although the raw data do identify some local abundance hotspots for ErM

521 (Figure S1). As a result, we focus the remainder of results and discussion on the three major tree

522 symbiotic states (EM, AM, N-fixer). Despite the fact that data from N. and S. America constitute

523 65% of the training data (at the 1 by 1 degree grid scale), our models accurately predict the

524 proportional abundances of the three major symbioses across all major geographic regions

525 (Figure S10). The high performance of our models, which is robust to both K-fold cross-

526 validation and rarefying samples so that all continents are represented with equal depth (Figures

527 S11-12), suggest that regional variations in climate (including indirect effects on decomposition)

528 and soil pH (for N-fixers) are the primary factors influencing the relative dominance of each

529 guild at the global scale (geographic origin only explained ~2-5% of the variability in residual

530 relative abundance) (Table S8, Figure S10).

531   Whereas a recent global analysis of root traits concluded that plant evolution has favored

532 reduced dependence on mycorrhizal fungi[21], we find that trees associating with the relatively

533 more C-demanding and recently-derived EM fungi[12,14] represent the dominant tree-symbiosis.

534 By taking the average proportion of EM trees, weighted by spatially-explicit global predictions

535 for tree stem density[11], we estimate that approximately 60% of trees on earth are EM, despite the

536 fact that only 2% of plant species associate with EM fungi (vs. 80% associating with AM fungi)[7].

537 Outside of the tropics, the estimate for EM relative abundance increases to approximately 80%

538 of trees.

539   Turnover among the major symbiotic guilds results in a tri-modal latitudinal abundance

540 gradient, with the proportion of EM trees increasing (and AM trees decreasing) with distance

541 from the equator, while the upper-quantiles of N-fixing trees reach peak abundance in the arid

542 zone around 30 degrees (Figure 3A, Figure 4). These trends are driven by abrupt transitional

543 regions along continental climatic gradients (Figure 2), which skew the distribution of symbioses

544 among biomes (Figure 3A) and drive strong patterns across geographic and topographic features

545 that influence climate. Moving north or south from the equator, the first transitional zone

546 separates warm (aseasonal), AM-dominated, tropical broadleaf forests (>75% median basal area,

547 vs. 8% for EM trees) from the rest of the EM-dominated world forest system (Figure 2AB;

548 Figure 3A). The transition zone occurs across the globe around 25 degrees N and S latitude, just

549 beyond the dry tropical broadleaf forests (with 25% EM tree basal area; Figure 3A), where

550 average monthly temperature variation reaches 3-5°C (temperature seasonality, Figure 2AB).

551   Moving further N or S, the second transitional climate zone separates regions where

552 decomposition coefficients during the warmest quarter of the year are less than 2 (see Figure 3B

553 for the associated temperature and precipitation ranges). In N. America and China, this transition

554 zone occurs around 50 degrees N, separating the mixed AM / EM temperate forests from their

555 neighboring EM dominated boreal forests (75 vs 100% EM tree basal area, respectively; Figure

556 3A). This transitional decomposition zone bypasses W. Europe, which has temperature

557 seasonality > 5°C, but lacks sufficiently wet summers to accelerate decomposition coefficients

558 beyond values associated with mixed AM/EM forests. The latitudinal transitions in symbiotic

559 state observed among biomes are mirrored by within-biome transitions along elevation gradients.

560 For example, in tropical Mexico, warm and wet quarter decomposition coefficients < 2 occur

561 along the slopes of the Sierra Madre, where mixed AM-exclusive and N-fixer woodlands in arid

562 climates transition to EM dominated tropical coniferous forests (75% basal area, Figure 3A,

563 Figure 4ABC, Figure S16-18). The southern hemisphere, which lacks the landmass to support

564 extensive boreal forests, experiences a similar latitudinal transition in decomposition rates along

565 the ecotone separating its tropical and temperate biomes, around 28 degrees S.

566   The abrupt transitions that we detected between forest symbiotic states along

567 environmental gradients suggest that positive feedbacks may exist between climatic and

568 biological controls of decomposition[10,20]. In contrast to AM fungi, some EM fungi can use

569 oxidative enzymes to mineralize organic nutrients from leaf litter, converting nutrients to plant-

570 usable forms[2,5]. Relative to AM trees, the leaf litter of EM trees is also chemically more resistant

571 to decomposition, with higher C:N ratios and higher concentrations of decomposition-inhibiting

572 secondary compounds[10]. Thus, EM leaf litter can exacerbate climatic barriers to decomposition,

573 promoting conditions where EM fungi have superior nutrient-acquiring abilities to AM-fungi[5,10].

574 A recent game theoretical model has shown that positive plant-soil-nutrient feedbacks can lead to

575 local bistability in mycorrhizal symbiosis[22]. Such positive-feedbacks are also known to cause

576 abrupt ecosystem transitions along smooth environmental gradients between woodlands and

577 grasses: trees suppress fires, which promotes seedling recruitment, while grass fuels fires, which

578 kill tree seedlings[23]. The existence of abrupt transitions also suggests that forests in transitional

579   regions along decomposition gradients should be susceptible to drastic turnover in symbiotic

580   state with future environmental changes[23].

581   To illustrate the sensitivity of global patterns of tree symbiosis to climate change, we use

582   the relationships we developed for current climate to project potential changes in forest

583   symbiotic status in the future. Relative to our global predictions using the most recent climate

584   data, model predictions using the projected climates for 2070 suggest the abundance of EM trees

585   will decline by as much as 10% (using a relative concentration pathway of 8.5 W/m^2; Figure

586   S24). Due to their position along decomposition gradients relative to the abrupt shift from EM to

587   AM forests (Figure 2AB), our models predict the largest declines in EM abundance will occur

588   along the boreal-temperate ecotone, although this model does not estimate the time lags between

589   climate change and forest community responses. The predicted decline in EM trees corroborates

590   the results of common garden transfer and simulated warming experiments, which demonstrate

591   that some important EM hosts will decline at the boreal-temperate ecotone in altered climates[24].

592   The change in dominant nutrient exchange symbioses along climate gradients highlights

593   the interconnection between atmospheric and soil compartments of the biosphere. The transition

594   from AM to EM dominance corresponds with a shift from P to N limitation of plant growth with

595   increasing latitude[25,26]. Including published global projections of total soil N or P, microbial N,

596   or soil P fractions (labile, occluded, organic, and apatite) did not increase the amount of variation

597   explained by the model or alter the variables identified as most important, and thus were dropped

598   from our analysis. However, our finding that climatic controls of decomposition best predict the

599   dominant mycorrhizal associations mechanistically links symbiont physiology with climatic

600   controls of soil nutrient release from leaf litter. These findings are consistent with Read's

601   hypothesis[16] that slow decomposition at high latitudes favors EM fungi due to their increased

602 capacity to liberate organic nutrients[2]. Thus, while more experiments are necessary to understand

603 the specific mechanism by which nutrient competition favors dominance of AM or EM

604 symbioses[18], we propose that the latitudinal and elevational transitions from AM to EM

605 dominated forests be called Read's Rule.

606   While our analyses focus on prediction at large spatial scales appropriate to the available

607 data, our findings with respect to Read's Rule also provide insight into how soil factors structure

608 the fine-scale distributions of tree symbioses within our grid cells. For example, while at a coarse

609 scale we find that EM trees are relatively rare in many wet tropical forests, individual tropical

610 sites in our raw data span the full range from 0 – 100 % EM basal area. In much of the wet

611 tropics, these EM dominated sites exist as outliers within a matrix of predominantly AM trees. In

612 an apparent exception that proves Read's Rule, in aseasonal warm neotropical climates, which

613 accelerate leaf-decomposition and promote regional AM dominance (Figure 3), EM dominated

614 tree stands can develop in sites where poor soils and recalcitrant litter slow decomposition and N

615 mineralization[18,27]. Landscape-scale variation in the relative abundance of symbiotic states also

616 changes along climate gradients, with variability highest in xeric and temperate biomes (Figure

617 S3-4), suggesting that the potential of local nutrient variability to favor particular symbioses is

618 contingent on climate.

619   Whereas EM trees are associated with ecosystems where plant growth is thought to be

620 primarily N-limited, N-fixer trees are not. Our results highlight the global extent of the "N-

621 cycling paradox," wherein some metrics suggest that N-limitation is greater in the temperate

622 zone[25,26], yet N-fixing trees are relatively more common in the tropics[15,28] (Figure 3A). We find

623 that N-fixers, which we estimate represent 7% of all trees, dominate forests with annual max

624 temperatures >35°C and alkaline soils (particularly in North America and Africa, Figure 2C).

625 They have the highest relative abundance in xeric shrublands (24%), tropical savannas (21%),

626 and dry broadleaf forest biomes (20%), but are nearly absent from boreal forests (<1%) (Figure

627 3A, Figure 4). The decline in N-fixer tree abundance we observed with increasing latitude is also

628 associated with a previously documented latitudinal shift in the identity of N-fixing microbes,

629 from facultative N-fixing rhizobial bacteria in tropical forests to obligate N-fixing actinorhizal

630 bacteria in temperate forests[28]. Our data are not capable of fully disentangling the several

631 hypotheses that have been proposed to reconcile the N-cycling paradox[15]. However, our results

632 are consistent with the model prediction[17] and regional empirical evidence[19,29,30] that N-fixing

633 trees are particularly important in arid biomes. Based primarily on the observed positive,

634 nonlinear association of N-fixer relative abundance with the mean temperature of the hottest

635 month (Figure 2C), our models predict a two-fold increase in N-fixer relative abundance when

636 transitioning from humid to dry tropical forest biomes (Figure 3A).

637 Although soil microbes are a dominant component of forests, both in terms of diversity

638 and ecosystem functioning[5,6,10], identifying global-scale microbial biogeographic patterns

639 remains an ongoing research priority. Our analyses confirm that Read's Rule, which is one of the

640 first proposed biogeographic rules specific to microbial symbioses, successfully describes global

641 transitions between mycorrhizal guilds. More generally, climate driven turnover among the

642 major plant-microbe symbioses represents a fundamental biological pattern in the Earth system,

643 as forests transition from low-latitude arbuscular mycorrhizal, to N-fixer, to high-latitude

644 ectomycorrhizal ecosystems. The predictions of our model (which we make available as a global

645 raster layer) can now be used to represent these critical ecosystem variations in global

646 biogeochemical models used to predict climate-biogeochemical feedbacks within and between

647 trees, soils, and the atmosphere. Additionally, the layer containing the proportion of N-fixing

648 trees can be used to map potential symbiotic N-fixation, which links together atmospheric pools

649 of C and N. Future work can extend our findings to incorporate multiple plant growth forms and

650 non-forested biomes, where similar patterns likely exist, to generate a complete global

651 perspective. Our predictive maps leverage the most comprehensive global forest dataset to

652 generate the first quantitative global map of forest tree symbioses, demonstrating how nutritional

653 mutualisms are coupled with the global distribution of plant communities.

654 **References**

655 1   Batterman, S. A. *et al.* Key role of symbiotic dinitrogen fixation in tropical forest
656   secondary succession. *Nature* **502**, 224-227, doi:10.1038/nature12525 (2013).
657 2   Shah, F. *et al.* Ectomycorrhizal fungi decompose soil organic matter using oxidative
658   mechanisms adapted from saprotrophic ancestors. *New Phytol* **209**, 1705-1719,
659   doi:10.1111/nph.13722 (2016).
660 3   Averill, C., Turner, B. L. & Finzi, A. C. Mycorrhiza-mediated competition between
661   plants and decomposers drives soil carbon storage. *Nature* **505**, 543-+,
662   doi:10.1038/nature12901 (2014).
663 4   Clemmensen, K. E. *et al.* Roots and associated fungi drive long-term carbon
664   sequestration in boreal forest. *Science* **339**, 1615-1618, doi:10.1126/science.1231923
665   (2013).
666 5   Cheeke, T. E. *et al.* Dominant mycorrhizal association of trees alters carbon and nutrient
667   cycling by selecting for microbial groups with distinct enzyme function. *New Phytol.*
668   **214**, 432-442, doi:10.1111/nph.14343 (2017).
669 6   Terrer, C., Vicca, S., Hungate, B. A., Phillips, R. P. & Prentice, I. C. Mycorrhizal
670   association as a primary control of the CO2 fertilization effect. *Science* **353**, 72-74,
671   doi:10.1126/science.aaf4610 (2016).
672 7   Brundrett, M. C. in *Biogeography of Mycorrhizal Symbiosis*   533-556 (Springer, 2017).
673 8   Averill, C. & Hawkes, C. V. Ectomycorrhizal fungi slow soil carbon cycling. *Ecol Lett*
674   **19**, 937-947, doi:10.1111/ele.12631 (2016).
675 9   Bennett, J. A. *et al.* Plant-soil feedbacks and mycorrhizal type influence temperate forest
676   population dynamics. *Science* **355**, 181-184 (2017).
677 10   Phillips, R. P., Brzostek, E. & Midgley, M. G. The mycorrhizal-associated nutrient
678   economy: a new framework for predicting carbon-nutrient couplings in temperate forests.
679   *New Phytol.* **199**, 41-51, doi:10.1111/nph.12221 (2013).
680 11   Crowther, T. W. *et al.* Mapping tree density at a global scale. *Nature* **525**, 201 (2015).
681 12   Heijden, M. G., Martin, F. M., Selosse, M. A. & Sanders, I. R. Mycorrhizal ecology and
682   evolution: the past, the present, and the future. *New Phytol.* **205**, 1406-1423 (2015).
683 13   Binkley, D., Sollins, P., Bell, R., Sachs, D. & Myrold, D. Biogeochemistry of adjacent
684   conifer and alder☐conifer stands. *Ecology* **73**, 2022-2033 (1992).

685   14   Leake, J. *et al.* Networks of power and influence: the role of mycorrhizal mycelium in
686   controlling plant communities and agroecosystem functioning. *Canadian Journal of*
687   *Botany* **82**, 1016-1045 (2004).
688   15   Hedin, L. O., Brookshire, E. N. J., Menge, D. N. L. & Barron, A. R. in *Annual Review of*
689   *Ecology Evolution and Systematics* Vol. 40 *Annual Review of Ecology Evolution and*
690   *Systematics*   613-635 (Annual Reviews, 2009).
691   16   Read, D. J. Mycorrhizas in Ecosystems. *Experientia* **47**, 376-391, doi:Doi
692   10.1007/Bf01972080 (1991).
693   17   Houlton, B. Z., Wang, Y.-P., Vitousek, P. M. & Field, C. B. A unifying framework for
694   dinitrogen fixation in the terrestrial biosphere. *Nature* **454**, 327 (2008).
695   18   Peay, K. G. The mutualistic niche: mycorrhizal symbiosis and community dynamics.
696   *Annual Review of Ecology, Evolution, and Systematics* **47**, 143-164 (2016).
697   19   Pellegrini, A. F., Staver, A. C., Hedin, L. O., Charles☐Dominique, T. & Tourgee, A.
698   Aridity, not fire, favors nitrogen☐fixing plants across tropical savanna and forest biomes.
699   *Ecology* **97**, 2177-2183 (2016).
700   20   Tuomi, M. *et al.* Leaf litter decomposition—estimates of global variability based on
701   Yasso07 model. *Ecological Modelling* **220**, 3362-3371 (2009).
702   21   Ma, Z. *et al.* Evolutionary history resolves global organization of root functional traits.
703   *Nature* (2018).
704   22   Lu, M. & Hedin, L. O. Global plant–symbiont organization and emergence of
705   biogeochemical cycles resolved by evolution-based trait modelling. *Nature ecology &*
706   *evolution*, 1 (2019).
707   23   Scheffer, M., Carpenter, S., Foley, J. A., Folke, C. & Walker, B. Catastrophic shifts in
708   ecosystems. *Nature* **413**, 591 (2001).
709   24   Reich, P. B. *et al.* Geographic range predicts photosynthetic and growth response to
710   warming in co-occurring tree species. *Nature Climate Change* **5**, 148 (2015).
711   25   McGroddy, M. E., Daufresne, T. & Hedin, L. O. Scaling of C: N: P stoichiometry in
712   forests worldwide: Implications of terrestrial redfield☐type ratios. *Ecology* **85**, 2390-
713   2401 (2004).
714   26   Reich, P. B. & Oleksyn, J. Global patterns of plant leaf N and P in relation to temperature
715   and latitude. *Proceedings of the National Academy of Sciences of the United States of*
716   *America* **101**, 11001-11006 (2004).
717   27   Corrales, A., Mangan, S. A., Turner, B. L. & Dalling, J. W. An ectomycorrhizal nitrogen
718   economy facilitates monodominance in a neotropical forest. *Ecol Lett* **19**, 383-392,
719   doi:10.1111/ele.12570 (2016).
720   28   Menge, D. N., Lichstein, J. W. & Ángeles-Pérez, G. Nitrogen fixation strategies can
721   explain the latitudinal shift in nitrogen☐fixing tree abundance. *Ecology* **95**, 2236-2245
722   (2014).
723   29   Liao, W., Menge, D. N., Lichstein, J. W. & Ángeles☐Pérez, G. Global climate change
724   will increase the abundance of symbiotic nitrogen☐fixing trees in much of North
725   America. *Global Change Biol* (2017).
726   30   Gei, M. *et al.* Legume abundance along successional and rainfall gradients in Neotropical
727   forests. *Nature ecology & evolution*, 1 (2018).
728

729   **Figure Legends**

730   **Figure 1. The global distribution of GFBi training data. The global map has n=2,768 grid**

731   **cells at a 1 x 1 degree latitude/longitude resolution. Cells are colored in the red, green and**

732   **blue spectrum according to the % of total tree basal area occupied by N-fixer, AM, and**

733   **EM tree symbiotic guilds, as indicated by the ternary plot. Grey cells show the global**

734   **distribution of forests where we make model projections.**

735

736   **Figure 2. A small number of environmental variables predict the majority of global**

737   **turnover in forest symbiotic status. Panels show the partial feature contrbutions of**

738   **different environmental variables on forest symbiotic state. Each row plots the shape of the**

739   **contribution of the four most important predictors of the proportion of tree basal area**

740   **belonging to the (a) ectomycorrhizal (EM), (b) arbuscular mycorrhizal (AM), and (c) N-**

741   **fixer symbiotic guilds (n=2,768). Variables are listed in declining importance from left to**

742   **right, as determined by inc node purity, with points colored with a red-green-blue gradient**

743   **according to their position on the x-axis of the most important variable (left-most panels**

744   **for each guild), allowing cross visualization between predictors. Each panel lists two**

745   **measures of variable importance, inc node purity (used for sorting) and %IncMSE (see**

746   **Supplemental Information for description). The abundance of each symbiont type**

747   **transitions sharply along climatic gradients, suggesting that sites near the threshold are**

748   **particularly vulnerable to switching their dominant symbiont guild with climate changes.**

749

750   **Figure 3. The distribution of forest symbiotic status across biomes is related to climatic**

751   **controls over decomposition. (a) Biome level summaries of the median +/- 1 quartile of the**

752   **predicted % tree basal area per biome for ectomycorrhizal (EM), arbuscular mycorrhizal**

753 **(AM), and N-fixer symbiotic guilds (n=100 random samples per biome). (b) The**

754 **dependency of decomposition coefficients (k, solid and dotted lines) on temperature and**

755 **precipitation during the warmest quarter with respect to predicted dominance of**

756 **mycorrhizal symbiosis. The transition from AM forests to EM forests between k=1 and 2 is**

757 **abrupt, which is consistent with positive feedback between climatic and biological controls**

758 **of decomposition.**

759

760 **Figure 4. Global maps of predicted forest tree symbiotic state. Maps (left) and latitudinal**

761 **gradients (right, with solid line indicating the median and colored ribbon spanning the**

762 **range from the 5% and 95% quantiles) of the % of tree basal area for (a) ectomycorrhizal**

763 **(EM), (b) arbuscular mycorrhizal (AM), and (c) N-fixer symbiotic guilds. All projections**

764 **are displayed a 0.5 by 0.5 degree lat/long scale with n=28,454.**

765 **Acknowledgements**

769 **Author Contributions**

770 KGP & TWC conceived the study; TWC, JL, PBR, GN, SdM, MZ, NP, BH, XZ, & CZ

771 conceived and organized the GFBi database; KGP, BSS, GDAW, & MVN compiled the

772 symbiosis database; BSS carried out the primary data analysis; MVN & DR contributed to data

773 compilation and analysis; BSS, TWC, MVN & KGP wrote the initial manuscript; BSS, TWC,

774 JL, MVN, GDAW, PBR, GN, SdM, MZ, NP, BH, XZ, CZ & KGP made substantial revisions to

775   all versions of the manuscript; all other named authors provided forest inventory data and

776   commented on the manuscript.

Data Availability

778   The GFBi database is available upon written request at https://www.gfbinitiative.org/datarequest.

779   Additionally, the symbiotic state assigned to tree species as a supplementary file, as are global

780   rasters of our model projections for EM, AM, and N-fixer proportion of tree basal area.

Conflict of Interest

782   The authors declare we have no conflict of interests.

Supplementary Information

784   For more information on symbiotic guild assignments, model selection, and supplementary

785   analyses, refer to SupplementaryInfo_Steidinger_etal2019.pdf. For the full suite of Supplemental

786   Files, including symbiotic guild assignments and rasters of model projections, refer to

787   SupplementalFiles_Steidinger_etal2019.zip

788

Methods

790   We quantified the relative abundance of tree symbiotic guilds across >1.1 million forest

791   census plots combined in the GFBi database, an extension from the plot-based Global Forest

792   Biodiversity (GFB[31]) database. The GFBi database consists of individual-based data that we

793   compiled from all the regional and national GFBi forest inventory data sets. The standardized

794   GFBi data frame, i.e. tree list, comprises tree ID, a unique number assigned to each individual

795   tree; plot ID, a unique string assigned to each plot; plot coordinates, in decimal degrees of

796   WGS84 datum; tree size, in diameter-at-breast-height; trees-per-hectare expansion factor; year of

797 measurement; data set name, a unique number assigned to each forest inventory data set; and

798 binomial scientific tree species names.

799   We error checked all species names from different forest inventory data sets in three

800 steps. First, we extracted scientific names from original data sets, keeping only the names of

801 genus and species (authority names are removed). Next, we compiled all the species names into

802 five general species lists, one for each continent. Finally, we verified individual species names

803 against 23 online taxonomic databases using the 'taxize' package of R programming language[32].

804 We assigned each morphospecies a unique name comprising the genus, the string "spp",

805 followed by the data set name and a unique number for that species. For example, "Picea

806 sppCNi1" and "Picea sppCNi2" represent two different species under the genus "Picea",

807 observed in the first Chinese data set (CNi).

808   We derived plot-level abundance information in terms of species abundance matrices.

809 Each species abundance matrix consisted of the number of individuals by species (column

810 vectors) within individual sample plots (row vectors). In addition, key plot-level information was

811 also added to the matrices, including plot ID, data set name, plot coordinates, the year of

812 measurement, and basal area, i.e. the total cross-sectional areas (m^2) of living trees per one

813 hectare of ground area.

814   Tree genera were assigned to a plant family using a plant taxonomy lookup table

815 generated by Will Cornwell (hosted on Github https://github.com/traitecoevo/taxonlookup),

816 which uses the accepted taxonomy from "The Plant List." The majority (96.5%) of genera from

817 the GFBi species were successfully matched to family; for those that could not be assigned, we

818 manually checked the GFBi genus and species against synonyms from The Plant List. Of the

819 remaining 1,038 mismatches, an additional 440 were assigned to family either by updating older

820   genera and species names with their more recent synonyms or else by correcting obvious

821   misspellings. The remaining 598 entries that could not be matched to family were excluded from

822   analysis.

823   We used a taxonomically-informed approach to assign symbiotic states to plant species

824   from the GFBi. Plant species were assigned to one of 5 symbiotic guilds – ectomycorrhizal

825   (EM), arbuscular mycorrhizal (AM), ericoid mycorrhizal (ErM), weakly AM or non-mycorrhizal

826   (AMNM), or N-fixer (Table S1). Although we did not model the relative abundance of ErM

827   trees, due to their rarity, we have included a map of their relative abundance from our grid

828   (Figure S1). We also include as a supplementary file the full species list, which includes columns

829   used to assign species to guild. In addition, we include here a list of families and genera assigned

830   to all guilds except AM (Tables S2-5) with notes for cases of species from individual genera that

831   were either assigned to two guilds simultaneously (e.g., *Alnus* is an N-fixer and EM) or where

832   species from individual genera were split between two different guilds (e.g., some *Pisonia* sp. are

833   weakly AM and some are EM). An AM summary table is excluded for length considerations—

834   the same information is available in the Supplementary File "SymbioticGuildAssignment.csv".

835   The taxonomy of species in our inventory was compared with recently published

836   literature on the evolutionary history of mycorrhizal symbiosis[7,33,34] and N-fixation[35-38]. Most

837   species symbiotic status could be reliably assigned at the genus (e.g. *Dicymbe*) or family level

838   (e.g. Pinaceae). For the few groups where status was unreliable or variable within a genus (e.g.

839   *Pisonia*) we conducted additional literature searches.

840   We assigned species to the EM category in three stages. First, at the family level (e.g.,

841   Pinaceae); next, as the genus level (e.g., Dicymbe); and finally, using literature searches for

842   unclear genera. For example, for the genus *Pisonia*, some species are AM and others are EM. We

843   used a published list from Hayward & Hynson (2014)[39] to sort species into the appropriate guild.

844   For the genus *Acacia*, we followed Brundrett (2017)[7] in assuming that only endemic Australian

845   species associate with EM, while all others are AM (we sorted *Acacia* species according to

846   provenance using http://worldwidewattle.com/).

847   The AMNM category lumped together all genera of terrestrial, non-epiphytic plants that

848   either lack arbuscular mycorrhizal fungi (AMF), or have low or inconsistent records of AMF

849   colonization of roots. For example, although there are some published records of AMF

850   colonization in the roots of Proteaceae, these records are inconsistent, and colonization is

851   generally low. Further, as Proteaceae are associated with a non-mycorrhizal root morphology

852   (the "cluster" or "proteoid root system") that allows them to access otherwise unavailable forms

853   of soil nutrients[40], we placed the entire family within AMNM. The family Urticaceae, which we

854   also characterized as AMNM, was somewhat problematic – early-successional species from

855   tropical forests, such as those in the genus *Cecropia*, have records of both low and absent AMF

856   colonization[41]. Our approach was to use the most broadly inclusive AMNM categorization.

857   N-fixer status was assigned at the genus level, using previously compiled databases of

858   global symbiotic N_2-fixation[35-38]. Given that symbiotic N_2-fixation with rhizobial or *Frankia*

859   bacteria has only evolved in four orders (Rosales, Cucurbitales, Fabales and Fagales)[42], all

860   species outside of this nitrogen-fixing clade were assigned non-fixing status. Some species could

861   not be assigned a N-fixer status because they were typed to a higher taxonomic level (e.g.

862   family) that is ambiguous from a N-fixer status perspective. We recorded when our assignment

863   of N-fixer status was based on phylogenetic criteria but where symbiotic N-fixation is

864   evolutionarily labile. Since these cases are more likely to be misassigned we excluded them from

865   the N-fixation category. The N-fixer group contains species that are colonized by AMF (e.g.,

866   most genera from Leguminosae) and others that are colonized by ectomycorrhizal fungi (e.g.,

867   *Alnus* sp.).

868   Most plant species form AM symbiosis, which is the basal symbiotic state to the later

869   derived EM and N-fixing symbioses. Further, many EM and N-fixing plants maintain the ability

870   to form AM symbiosis. Thus, a tree species is most likely AM if it does not form associations

871   with another symbiotic guild (or forgoes root symbiosis entirely), as evidenced by their inclusion

872   in exhaustive databases of plant symbiotic state[7,33-38,41]. In keeping with other large-scale studies

873   in the field (e.g. [34]), we assigned tree species from the GFBi database to an AM-exclusive state if

874   they belonged to taxa that were not matched to EM, ErM, non-or-weakly mycorrhizal or N-fixer

875   symbioses. Thus, the AM and N-fixer groups in our dataset are non-overlapping despite the fact

876   that most N-fixers also associate with AM fungi.

877   The proportions of tree basal area and tree individuals were aggregated to a 1' by 1'

878   degree grid by taking the weighted average of the plot-level proportions (Table S6). This resulted

879   in a total of 2,768 grid cells, each with a score for the proportional abundance of EM, AM, N-

880   fixer, ErM, and AMNM trees. We calculated two measures of relative abundance for each

881   symbiotic guild: proportion of tree stems and proportion of tree basal area. Because the

882   measurements are highly correlated with one another (Figure S2) we chose to model only

883   proportion of total tree basal area, which should scale more approximately to proportion of tree

884   biomass as it accounts for differences in size among individual stems. Additionally, we

885   quantified variability among plots within each grid cell by calculating the weighted standard

886   deviation across the grid (Supplemental Information, Figure S3-4).

887   To identify the key factors structuring symbiotic distributions we assembled 70 global

888   predictor layers: 19 climatic (annual, monthly, and quarterly temperature and precipitation

889   variables), 14 soil chemical (total soil N density, microbial N, C:N ratios and soil P fractions,

890   pH, cation exchange capacity), 5 soil physical (soil texture and bulk density), 26 vegetative

891   indices (leaf area index, total stem density, enhanced vegetation index means and variances), and

892   5 topographic variables (elevation, hillshade) (Table S7). Because decomposition is the dominant

893   process by which soil nutrients become available to plants, we generated 5 additional layers that

894   estimate the climatic control of decomposition. We parameterized decomposition coefficients

895   according to the Yasso07 model[20,43] using the following equation:

896
$$k = \text{Exp}(0.095T_i - 0.00014\ T_i^2)\ (1\text{-Exp}[\ \text{-}1.21\ P_i]), \tag{1}$$

897   where P_i and T_i are precipitation and mean temperature, either quarterly or annually, and the

898   constants 0.0095 ($=\beta_1$) -0.00014 ($=\beta_2$) , and -1.21 ($=\gamma$) are parameters fit using a previous global

899   study of leaf litter mass-loss[20]. Although local decomposition rates can vary significantly based

900   on litter quality or microbial community composition[44], climate is the primary control at the

901   global scale[20]. Decomposition coefficients describe how fast different chemical pools of leaf

902   litter lose mass over time relative to a parameter, α, that accounts for leaf-chemistry.

903   Decomposition coefficients (k) with values of 0.5 and 2 indicate a halving and doubling of

904   decomposition rates relative to α, respectively (Supplemental Information, Figure S5).

905   We implemented the random forest algorithm using the "randomForest" packaged in R.

906   Random forest models average over multiple regression trees, each of which uses a random

907   subset of all the model variables to predict a response. We first determined the influence and

908   relationship of all 75 predictor layers on forest symbiotic state and then optimized our models

909   using a stepwise reduction in variables, from least- to most-important. Variable importance was

910   measured in two ways: Inc Node Purity and %IncMSE (with values reported in each panel of

911   Figure 2). The inc node purity of variable x considers the decrease in the residual sum of squares

912   that results from splitting regression trees using variable x. %IncMSE (mean square error)

913   quantifies the increase in model error as a result of randomly shuffling the order of values in the

914   vector x. We chose to rank variables according to inc node purity because we found that higher

915   inc node purities were associated with larger effect sizes, whereas larger %IncMSE were

916   associated with more linear responses of smaller effect. Whereas our inspection of partial feature

917   contributions is derived from univariate random forest models, we additionally ran multivariate

918   random forests the predict the proportional abundance of EM, AM, and N-fixer trees for each

919   pixel. The multivariate models were run using 50-regression trees each, with the unique set of the

920   best 4 predictor variables for each symbiotic guild in the univariate models (Table S7, Figure 2).

921   Despite strong negative correlations between the proportions of EM and AM basal area (Figure

922   S22), the results from multivariate and univariate random forests are strongly correlated with one

923   another (Figure S23).

924   Using model selection based on eliminating variables with low Inc Node Purity, we

925   removed most soil nutrient, vegetative, and topographic variables from our models (Figure S6-

926   7). Our final models include the remaining 34 predictor layers with climate, decomposition, and

927   certain soil physical and chemical information (Figure S8). To determine the parsimony of our

928   models, we compared the coefficient of determination in models run with a stepwise reduction in

929   the number of variables (starting with those with the lowest Inc Node Purity). Based on

930   performance of the ratio of coefficient of determination in models with 4 vs 34 variables, we

931   determined that the 4 most important variables accounted for >85% of the explained variability

932   (Figure S9). We also compared model performance visually with plots of actual vs predicted

933   proportions of each tree symbiotic guild among continents and geographic subregions (Figure

934   S10). We used the "forestFloor" packaged in R to plot the partial variable response of tree

935   symbiotic guilds to each predictor variable (Figure 2ABC, see Figure S19-21 for partial plots of

936   the partial feature contributions of all 34 variables).

937   In order to test the sensitivity of model performance and predictions, we performed cross

938   validation in R using the "rfUtilities" package[24]. K-fold cross validation tests the sensitivity of

939   model predictions to losing random subsets from the training data. For EM, AM, and N-fixer

940   models we ran 99 iterations that withheld 10% of the model training data. We assessed the drop

941   in model performance in the 99 iterations by manually calculating the coefficient of

942   determination, which uses the following formula: $1 - \Sigma$ (actual % basal area – predicted % basal

943   area)^2 / Σ (actual % basal area – mean actual % basal area)^2. For all symbiotic guilds,

944   withholding 10% of the training data resulted in a mean loss in variance explained of less than

945   1% (Figure S11). This shows that our training data has sufficient redundancy to ensure that our

946   model conclusions are robust. Similarly, to determine whether our random forest models would

947   make similar predictions if data were equally distributed among continents, we rarefied our

948   aggregated grid of symbiotic states and predictor layers to an even depth. Specifically, we sub-

949   sampled all continents – N. America (including Central America and the Caribbean), S. America,

950   Europe, Asia, and Oceania – to match the number of grid-pixels from Africa (n=50). This is a

951   much more aggressive reduction of training data than is typically used in K-fold cross

952   validations, as it involves dropping ~90% of training data rather than retaining the same amount.

953   We performed 99 iterations of rarefaction each for the three symbiotic guilds. On average,

954   models run with the rarefied data explained about 10% less variance over the full training data

955   (the entire predictor / response grid) than did models run with all of the training data (Figure

956   S12-13).

31

957   To avoid projecting our random forest models outside the ranges of their training data

958   (e.g., grid cells with higher mean annual temperatures than the maximum used to fit the models),

959   we subset a global grid of predictor layers depending on whether (1) the grid cell fell within the

960   top 60% of land surface with respect to tree stem density[11] and either (2) fell within the

961   univariate distribution of all the predictor layers from our training data and/or (3) fell within an

962   8-dimensional hypervolume defined by the unique set of the 4-best predictors of the relative

963   abundance of each guild (Figure S14). We then projected our models across only those grid cells

964   that met these criteria, which constitutes 46% of the global land surface and 88% of global tree

965   stems (Figure 1; Figure S15). Model projections were made at two resolutions: both 1 by 1

966   degree and 0.5 by 0.5 degree resolution (Figure 4). While model validation indicates that our

967   projections are robust, additional ground truthing of predictions to identify any discrepancies

968   would be incredibly valuable. If such discrepancies exist they can help fine tune climate-

969   symbiosis models, or identify areas where climate might favour invasion by symbioses that have

970   not yet evolved or dispersed to a particular biogeographic region.

971   We used the following equation to estimate the % of global tree stems that belong to

972   each tree symbiotic guild: Σ_i (predicted proportion of trees of guild g in pixel i) x (total number

973   of tree stems in pixel i) / Σ_i (total number of tree stems in pixel i). The proportion of tree stems

974   and the proportion of tree basal area in each guild are highly correlated throughout the training

975   data (Figure S4). The figures cited in the main text for each guild were calculated using model

976   projections across all pixels, even those that did not meet the criteria for model projection

977   because they fell outside the multivariate distribution of the predictor layers or had insufficient

978   stem density. However, our estimates for the global % of trees occupied by each tree symbiotic

979   guild change by <1% when using only those pixels that met our criteria for model projection.

980   In the main manuscript we state that sharp transitions between dominant symbiotic states

981   with climate variables could lead to declines in EM trees, particularly in southern boreal forests.

982   To determine this, we projected our random forest models for each symbiotic guild using climate

983   change projections over our 19 bioclimatic variables (Table S7), including the decomposition

984   coefficients that use temperature and precipitation values. Specifically, we considered the 2070

985   scenario with a relative concentration pathway (RCP) of 8.5 (W/m^2), which predicts an increase

986   of greenhouse gas emissions throughout the 21st century[45]. We plot difference in the proportion

987   of forest basal area between the projections for 2070 and those using current climate data (Table

988   S7, Figure S24). We qualify this prediction with the note that vegetative changes to forests are

989   constrained by rates of mortality, recruitment, and growth.

990   After training and cross-validating our models with GFBi data exclusively, we

991   additionally tested whether our models accurately predicted the symbiotic state of Eurasian

992   forests previously published by Schepaschenko et al. (2017)[46]. We assigned symbiotic status to

993   all trees in Schepaschenko et al. (2017) and aggregated plot level data to a 1 by 1 degree grid

994   using the same methods as with the GFBi dataset (Figure S25). We found that, on average, our

995   models predicted the symbiotic state in the regional dataset within 13.6% of the value of this

996   other dataset (Figure S26). For projected maps in Figure 4abc, we included the Schepaschenko et

997   al. (2017) data with the GFBi training data to increase geographic coverage throughout Eurasia.

998

999   **Methods References**

1000
1001   31   Liang, J. *et al*. Positive biodiversity-productivity relationship predominant in global
1002   forests. *Science* **354**, aaf8957 (2016).
1003   32   Chamberlain, S. A. & Szöcs, E. taxize: taxonomic search and retrieval in R.
1004   *F1000Research* **2** (2013).

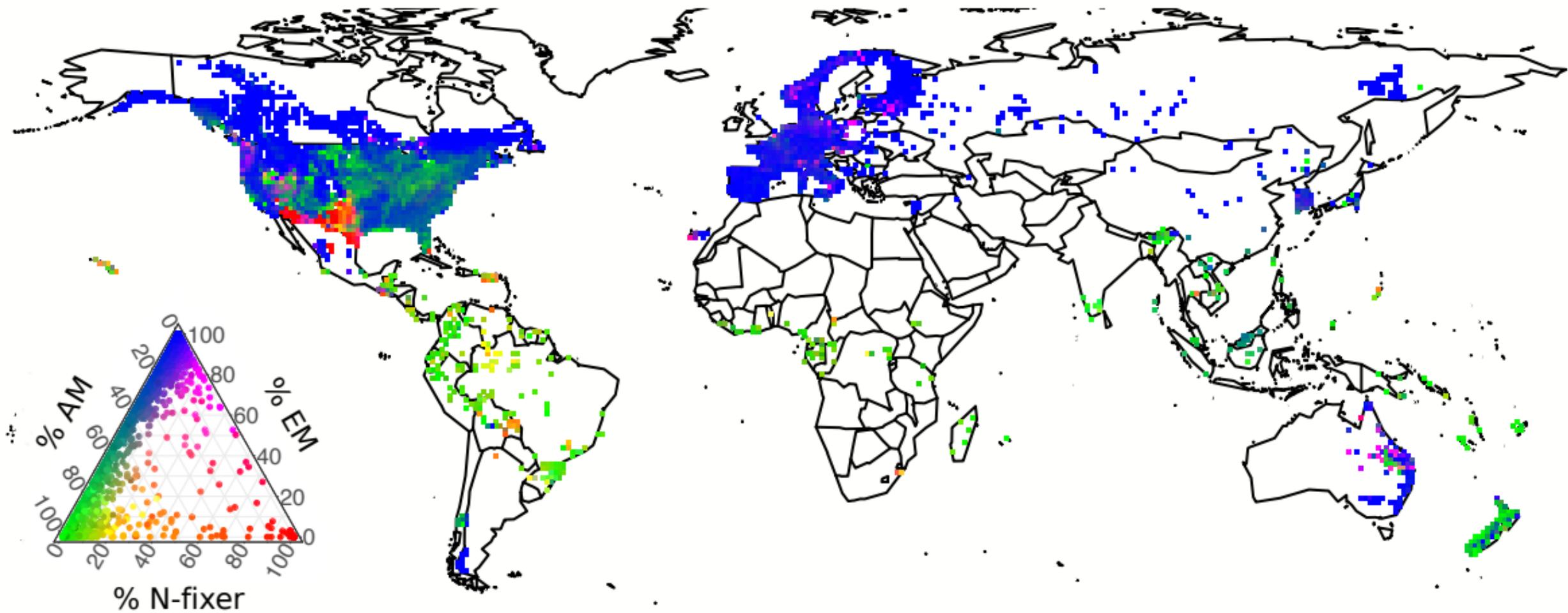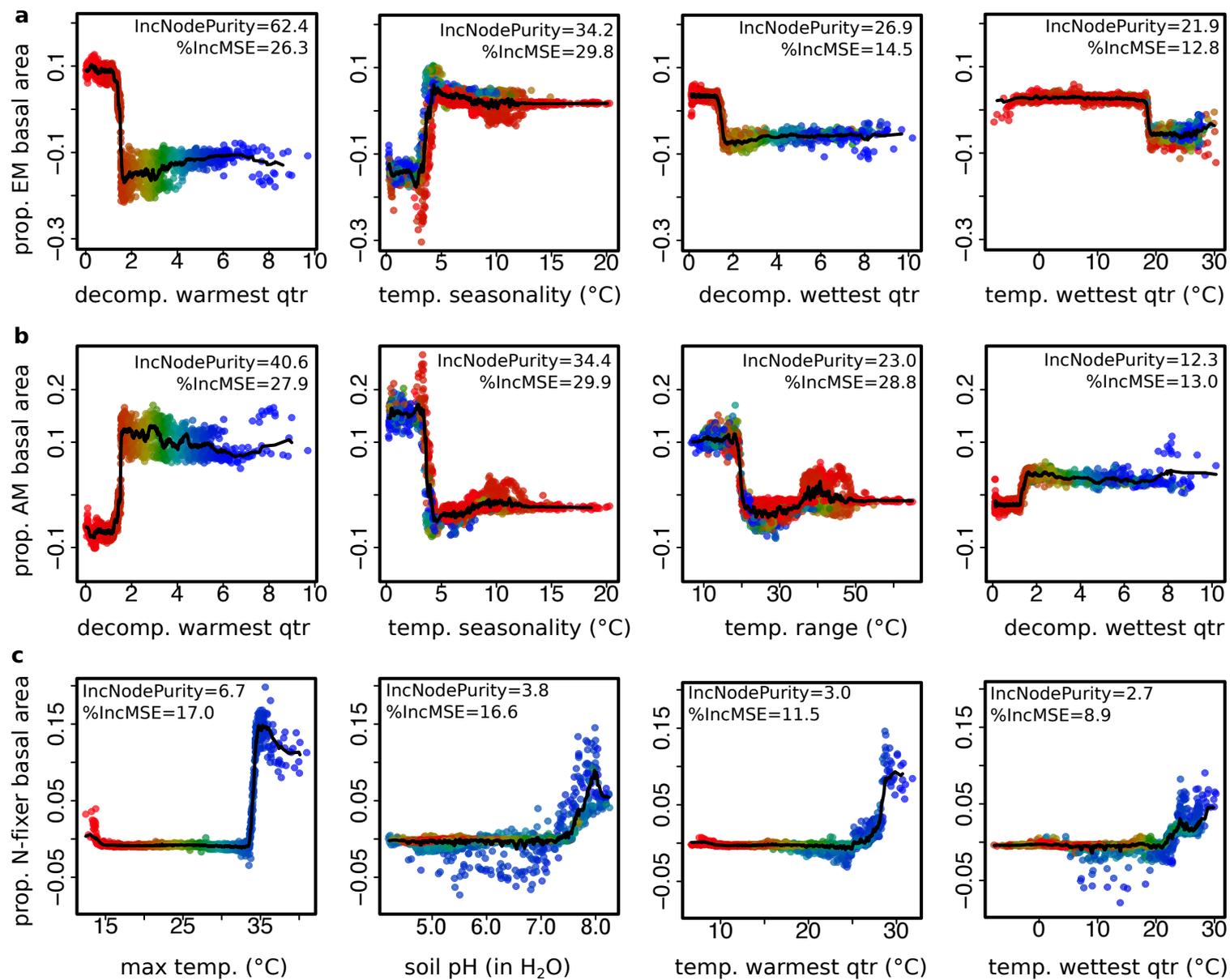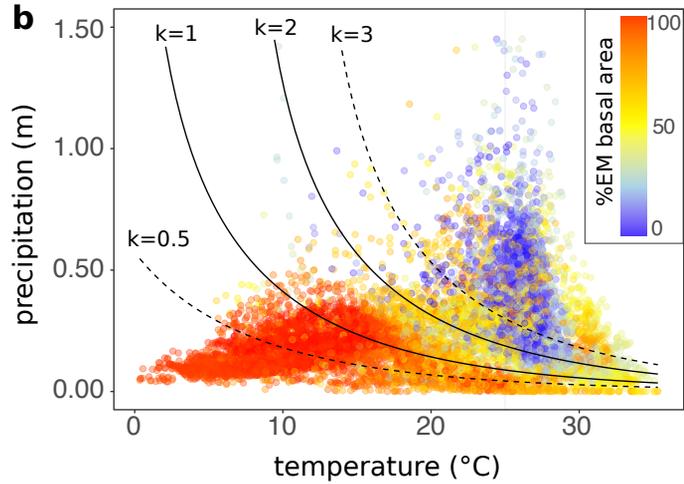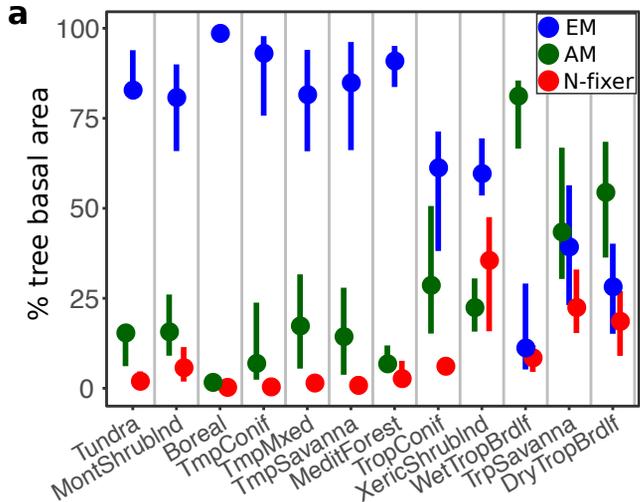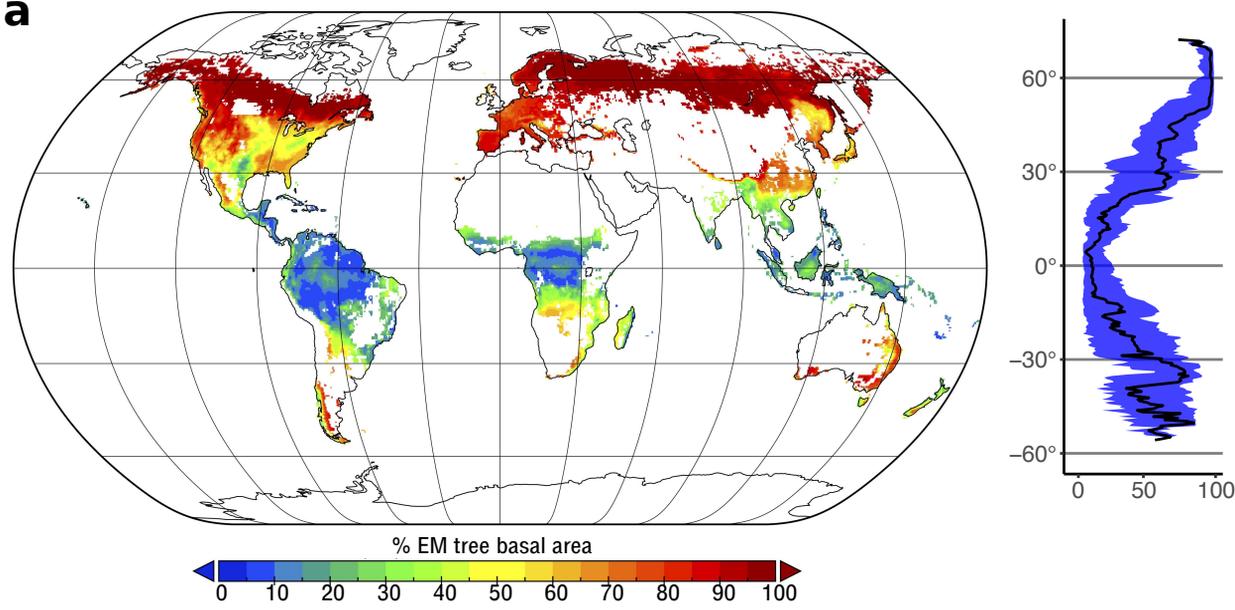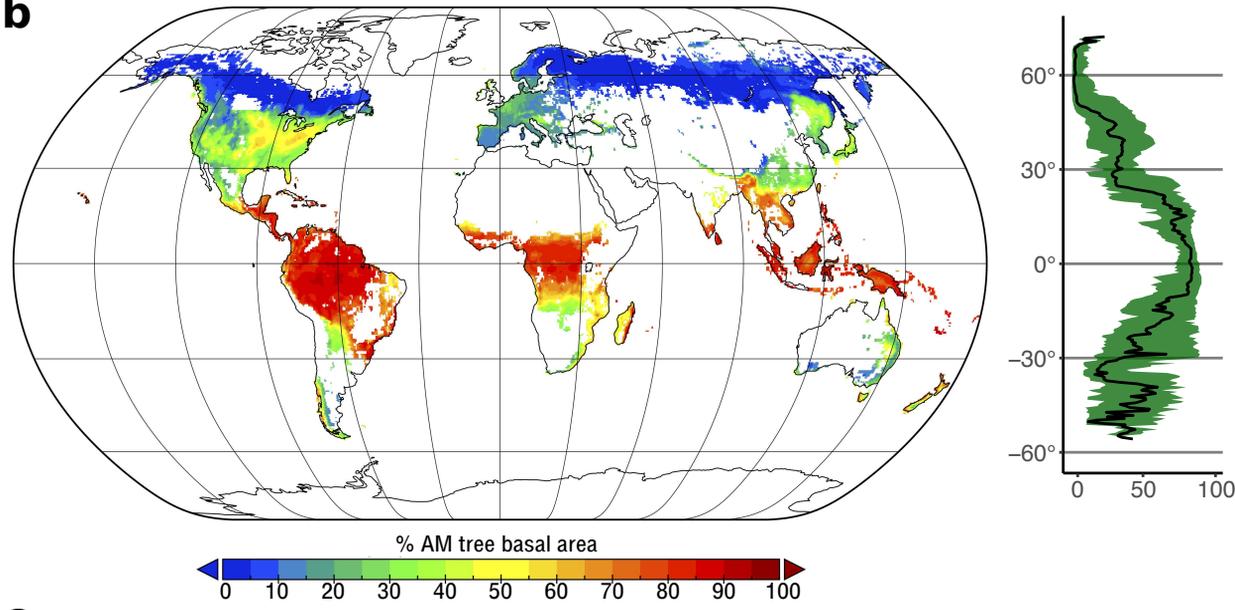| 1005 | 33 | Brundrett, M. C. & Tedersoo, L. Evolutionary history of mycorrhizal symbioses and |
1006		global host plant diversity. *New Phytol.* (2018).
1007	34	Brundrett, M. C. Mycorrhizal associations and other means of nutrition of vascular
1008		plants: understanding the global diversity of host plants by resolving conflicting
1009		information and developing reliable means of diagnosis. *Plant and Soil* **320**, 37-77,
1010		doi:10.1007/s11104-008-9877-9 (2009).
1011	35	Werner, G. D., Cornwell, W. K., Sprent, J. I., Kattge, J. & Kiers, E. T. A single
1012		evolutionary innovation drives the deep evolution of symbiotic N 2-fixation in
1013		angiosperms. *Nature Communications* **5**, 4087 (2014).
1014	36	Werner, G. D., Cornwell, W. K., Cornelissen, J. H. & Kiers, E. T. Evolutionary signals of
1015		symbiotic persistence in the legume–rhizobia mutualism. *Proceedings of the National*
1016		*Academy of Sciences* **112**, 10262-10269 (2015).
1017	37	Afkhami, M. E. *et al.* Symbioses with nitrogen☐fixing bacteria: nodulation and
1018		phylogenetic data across legume genera. *Ecology* **99**, 502-502 (2018).
1019	38	Tedersoo, L. *et al.* Global database of plants with root☐symbiotic nitrogen fixation: Nod
1020		DB. *Journal of Vegetation Science* (2018).
1021	39	Hayward, J. & Hynson, N. A. New evidence of ectomycorrhizal fungi in the Hawaiian
1022		Islands associated with the endemic host Pisonia sandwicensis (Nyctaginaceae). *Fungal*
1023		*Ecol* **12**, 62-69 (2014).
1024	40	Lambers, H., Martinoia, E. & Renton, M. Plant adaptations to severely phosphorus-
1025		impoverished soils. *Current opinion in plant biology* **25**, 23-31 (2015).
1026	41	Wang, B. & Qiu, Y.-L. Phylogenetic distribution and evolution of mycorrhizas in land
1027		plants. *Mycorrhiza* **16**, 299-363 (2006).
1028	42	Soltis, D. E. *et al.* Chloroplast gene sequence data suggest a single origin of the
1029		predisposition for symbiotic nitrogen fixation in angiosperms. *Proceedings of the*
1030		*National Academy of Sciences* **92**, 2647-2651 (1995).
1031	43	Palosuo, T., Liski, J., Trofymow, J. & Titus, B. Litter decomposition affected by climate
1032		and litter quality—testing the Yasso model with litterbag data from the Canadian intersite
1033		decomposition experiment. *Ecological Modelling* **189**, 183-198 (2005).
1034	44	Bradford, M. A. *et al.* Climate fails to predict wood decomposition at regional scales.
1035		*Nature Climate Change* **4**, 625 (2014).
1036	45	Allen, M. R. *et al.* IPCC fifth assessment synthesis report-climate change 2014 synthesis
1037		report. (2014).
1038	46	Schepaschenko, D. *et al.* A dataset of forest biomass structure for Eurasia. *Scientific data*
1039		**4**, 170070 (2017).
1040		

a (first row, prop. EM basal area)

Panel 1: IncNodePurity=62.4, %IncMSE=26.3 — decomp. warmest qtr
Panel 2: IncNodePurity=34.2, %IncMSE=29.8 — temp. seasonality (°C)
Panel 3: IncNodePurity=26.9, %IncMSE=14.5 — decomp. wettest qtr
Panel 4: IncNodePurity=21.9, %IncMSE=12.8 — temp. wettest qtr (°C)

b (second row, prop. AM basal area)

Panel 1: IncNodePurity=40.6, %IncMSE=27.9 — decomp. warmest qtr
Panel 2: IncNodePurity=34.4, %IncMSE=29.9 — temp. seasonality (°C)
Panel 3: IncNodePurity=23.0, %IncMSE=28.8 — temp. range (°C)
Panel 4: IncNodePurity=12.3, %IncMSE=13.0 — decomp. wettest qtr

c (third row, prop. N-fixer basal area)

Panel 1: IncNodePurity=6.7, %IncMSE=17.0 — max temp. (°C)
Panel 2: IncNodePurity=3.8, %IncMSE=16.6 — soil pH (in H_2O)
Panel 3: IncNodePurity=3.0, %IncMSE=11.5 — temp. warmest qtr (°C)
Panel 4: IncNodePurity=2.7, %IncMSE=8.9 — temp. wettest qtr (°C)

a

% EM tree basal area

0 10 20 30 40 50 60 70 80 90 100

b

% AM tree basal area

0 10 20 30 40 50 60 70 80 90 100

c

% N-fixer tree basal area

0 4 8 12 16 20 24 28 32 36 40